Development of Diamond Tracking Detectors for High Luminosity Experiments at the LHC

The RD42 Collaboration

W. Adam[1], C. Bauer[2], E. Berdermann[3], F. Bogani[4], E. Borchi[5], M. Bruzzi[5], C. Colledani[6],
J. Conway[7], W. Dabrowski[8], P. Delpierre[9], A. Deneuville[10], W. Dulinski[6], R. v. d. Eijk[11],
B. van Eijk[11], A. Fallou[9], D. Fish[7], M. Friedl[1], K.K. Gan[12], E. Gheeraert[10], E. Grigoriev[2],
G. Hallewell[9], R. Hall-Wilton[13], S. Han[14], F. Hartjes[11], J. Hrubec[1], D. Husson[6], H. Kagan[12,◇],
D. Kania[15], J. Kaplon[8], R. Kass[12], K.T. Knöpfle[2], M. Krammer[1], P.F. Manfredi[16], D. Meier[8],
F. LeNormand[6], L.S. Pan[17], H. Pernegger[1], M. Pernicka[1], R. Plano[7], V. Re[16], G.L. Riester[6], S. Roe[8],
D. Roff[13], A. Rudge[8], M. Schieber[17], S. Schnetzer[7], S. Sciortino[5], V. Speziali[16], H. Stelzer[3], R. Stone[7],
R.J. Tapper[13], R. Tesarek[7], G.B. Thomson[7], M. Trawick[12], W. Trischuk[18], R. Turchetta[6],
A.M. Walsh[7], P. Weilhammer[8,◇], H. Ziock[14], M. Zoeller[12]

[1] *Institut für Hochenergiephysik der Österr. Akademie d. Wissenschaften, A-1050 Vienna, Austria*
[2] *MPI für Kernphysik, D-69029 Heidelberg, Germany*
[3] *GSI, Darmstadt, Germany*
[4] *LENS, Florence, Italy*
[5] *University of Florence, Florence, Italy*
[6] *LEPSI, CRN, Strasbourg 67037, France*
[7] *Rutgers University, Piscataway, NJ 08855, U.S.A.*
[8] *CERN, CH-1211, Geneva 23, Switzerland*
[9] *CPPM, Marseille 13288, France*
[10] *LEPES, Grenoble, France*
[11] *NIKHEF, Amsterdam, Netherlands*
[12] *The Ohio State University, Columbus, OH 43210, U.S.A.*
[13] *Bristol University, Bristol BS8 1TL, U.K.*
[14] *Los Alamos National Laboratory, Research Division, Los Alamos, NM 87545, U.S.A.*
[15] *Lawrence Livermore National Laboratory, Livermore, CA 94550, U.S.A.*
[16] *Universita di Pavia, Dipartimento di Elettronica, 27100 Pavia, Italy*
[17] *Sandia National Laboratory, Livermore, CA 94550, U.S.A.*
[18] *University of Toronto, Toronto, ON M5S 1A7, Canada*

◇ Spokespersons

Abstract

The LHC which offers unique physics opportunities presents an extreme environment. As a result, tracking devices at the LHC need to have special properties. They must be radiation hard, provide fast collection of charge, be as thin as possible and be able to operate at reasonable temperatures. Moreover, it is becomming clear they should last a reasonable amount of time since replacement will be difficult. The properties of diamond allow it to fulfill these requirements and make it an ideal material for detectors in this high rate, high radiation environment. The RD42 collaboration program goal is to develop diamond detectors for the LHC. This work includes improving the charge collection properties of CVD diamond, studying the radiation hardness of the material and developing low noise radiation hard readout electronics suitable for use with diamond detectors. During the past year RD42 has made major progress on each of these fronts. As a result, the RD42 collaboration has grown in size adding the strength of four new groups. In this report we describe the progress we have made during the last year and outline the research program we intend to pursue in the future.

Contents

1   The RD42 1996 Research Program and Milestones

During the past year RD42 has continued to concentrate on improving the quality of chemical vapour deposition (CVD) diamond material for detector application. Having achieved a collection distance in excess of 100 μm in 1995 [1] our goal was to produce diamond material with a collection distance of 200 μm. As will be outlined below one manufacturer has recently reached this 200 μm milestone. We believe that having more than one manufacturer collaborating with us will make the eventual production of several square meters of diamond detector material for applications in LHC experiments an economically viable situation.

In addition we prepared a number of particle detectors based on our best material. We continue to benchmark new material with "slow" silicon detector readout chips, VA2 or VA3. These chips have a characteristic shaping time of 2 μs. Diamond material which has been successfully tested in this way is then re-patterned and connected to "fast" analogue readout electronics, SCT32A, which has a signal shaping time of 25 ns. As will be described in Sec. 5 we have for the first time successfully operated a prototype diamond tracker at a shaping time equal to the bunch crossing time in LHC experiments.

We have also concentrated on the development of pixel related diamond detectors to develop a proof-of-principle for this geometry. While readout electronics with sufficiently good performance for true bump-bonded diamond pixel detectors does not yet exist we have developed a glass fanout which routes signals from a 16 × 16 array of pixels with 150 μm pitch to the edges of the device. From there we have successfully read out the detector with VA3 electronics in a beam test as will be described in Sec. 4.2.

In the past year we also prepared particle detectors which were tested the first time in a magnetic field up to 3 T. This work is reported in Sec. 4.3.

Finally, we have continued our irradiation studies of CVD diamond having irradiated high quality diamond to doses corresponding to ten years of LHC operation. After irradiation with pions and neutrons with total fluences exceeding 10^{15} particles per cm^2 the diamond devices perform properly. This work will be described in Sec. 3.

1.1   The LDRB Milestones

The prime milestone, set in November 1995 by the LRDB, was the further improvement of CVD diamond material. The goal remained to reach 200 μm collection distances. We attacked this target on a number of fronts. As we reported last year [2], one manufacturer had already developed a process for growing diamond with a collection distance of 110 to 120 μm. There were two non-exclusive ideas on how to proceed. Both manufacturers attempted to reach the 200 μm collection distance goal by developing the chemistry of the growth process. This research showed promising results which we outlined in last year's status report [1]. However, it has not yet yielded a reliable set of growth parameters for either manufacturer. Apparently, while studies looked very promising on thin samples, the extension of the growth process to full thickness wafers involves non-trivial engineering. This work will be continued by both manufacturers in the next year as a method of reducing the cost of high quality diamond.

Our second manufacturer started out the year with material of 50 to 60 μm collection distance in isolated samples. They chose to grow thick samples since the collection distance in CVD diamond increases with the thickness of the material [3]. They made steady progress throughout the year culminating in a sample with a collection distance of 200 μm. This progress, though rapid, highlights the complexity of the task involved and the resources required on the part of a company to advance in this field. Our work together over the last two years has involved the testing of almost 70 small samples from at least 50 different diamond growths. Although we do not have detailed information on the growth parameters our estimate is that we tested

essentially all the output of one research reactor over this two year period.

Our second milestone was to further our tests of the radiation hardness of CVD diamond material. These studies had two foci. At the time of our last renewal it remained to fully understand and quantify the maximum exposure to neutrons that was possible without significant degradation of the charge collection distance. We have now finished the first round of these studies and sharpened our understanding. We show, below, that the detector quality of CVD diamond in the pumped-up state at room temperature is insensitive to neutrons up to fluences of 4×10^{14} per cm^2. Beyond this we observe a 25% decrease of the collection distance at fluences of 1.9×10^{15} per cm^2. We intend to extend studies up to fluences of 5×10^{15}, which represents the conditions just outside the beampipe. As this exceeds the doses expected in LHC experiments even at the smallest radii accessible we believe this fluence is sufficient to study radiation effects in diamond detectors. We continue to study the long term behavior of the samples exposed to the highest fluences and we plan to repeat these studies with higher collection distance samples as more of this material becomes available.

In addition to completing the first round of neutron studies we have continued our series of pion irradiations. Results are now available for pion fluences up to 5.6×10^{14} per cm^2 on the highest quality diamond available last year. In September of this year we have finally accumulated a dose of more than 10^{15} pions per cm^2 on our original samples after three pion exposures. This represents the full lifetime dose of pions expected on a diamond tracker at a radius of 10 cm in the LHC over a period of 10 years at full luminosity.

As part of the LDRB milestones we were encouraged to expand our understanding of the growth mechanisms of CVD diamond material. This involved characterising the material in ways beyond that of the collection distance which remains our prime characteristic. A number of studies have been carried out principally at LENS but also at LEPES/Grenoble, and Sandia National Lab. These studies have been aimed at improving the electrical contact to diamond and understanding the effect of neutron irradiation on the hydrogen content of the diamond. As we have yet to come to any conclusions on correlations between collection distance and these other parameters we have not included details in this report. The prime focus of this work, however has been to better understand the relationship between materials properties and the changes in collection distance associated with exposure to neutrons – the only source of particles to show any change of collection distance in the material.

The LDRB set three particle detector oriented milestones for the collaboration last year. The first of these centered on the desire to see what possible performance limitations might arise in the patterning of pixelated detector elements onto the CVD diamond substrates. As mentioned above, in the absence of suitable bump bonded pixel readout electronics, we have successfully fulfilled two thirds of the possible sub-milestones in this area. The electrode lithography presented no problems even on the fairly rough growth side of the diamond down to a scale of 150 $\times$ 150 μm^2 [Fig. 1]. In addition, there was no apparent loss of charge seen between the readout pads. It remains to be seen how these devices will perform with truly pixelated electronics.

The second detector milestone was to develop a prototype detector with a signal shaping time suitable for use at the LHC. Here we have been successful despite the lack of specific developments in frontend electronics for diamond sensors. We have been able to readout a diamond strip detector with an effective pitch of 100 μm using electronics that had an effective shaping time of 25 ns. These electronics were developed for the readout of silicon trackers and have not yet been adapted for the lower capacitance and leakage currents found in diamond sensors. We expect to be able to significantly improve on the results presented below by developing a chip dedicated for use with diamond sensors in the coming year.

Finally we were asked to consider the extension of our work to sensors of larger size than the 1 $\times$ 1 cm^2 currently in use. During the year we tested one 2 $\times$ 4 cm^2 sample and placed purchase orders of 3 additional pieces. The manufacturers claim that producing detectors this
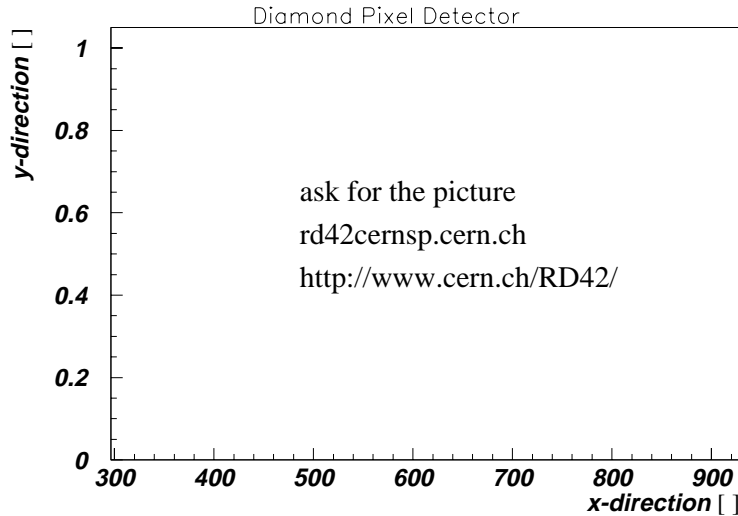
Figure 1: A photograph of the pixel detector described in the text on the growth side of a CVD diamond.

size is not a problem. The first 2×4 cm^2 sample was tested quite early in the year and it did not have sufficient collection distance for us to keep it. It has been returned. We still have outstanding orders for four 2×4 cm^2 detector pieces some of which we expect will be filled in early 1997. Thus we should be in a position to achieve this milestone in the course of the next year.

2   Progress on the Improvement of CVD Diamond

Two important developments occurred in the improvement of detector grade CVD diamond during the past year. The first development was the production of a CVD diamond with 200 μm collection distance; the second development was to help the second manufacturer produce high quality diamond with > 100 μm collection distance. To put these developments in perspective, when RD42 started nearly three years ago, the best available CVD diamond had a collection distance of 40 μm. In our last status report we showed that one manufacturer had produced diamond which reached a collection distance of 100 μm and a most probable signal of 2500 e.

During the past year we have worked closely with the manufacturers to determine just how to improve the quality of diamond. We have measured and characterised approximately 50 samples from over 30 different growth runs. We have given the results of our work to the manufacturers with the idea that they would correlate our results with their understanding of the growth parameters. The results of this work were:

- The development of a stable and for each manufacturer an individual process for producing as-grown CVD diamond with 125 μm collection distance corresponding to a most probable signal of 3400 e.

- A recipe for post processing the as-grown diamond to enhance the collection distance to 200 μm or 5400 e most probable signal.

The results of our work during the last year include the achievement of the same signal size (most probable signal of 2300 e) with a 50 μm pitch strip detector using fast electronics (22 ns) as we obtained with slow electronics (2 μs) indicating that the charge collection mechanism in

diamond is quite fast, and the production of the first diamond with 200 μm collection distance (most probable signal of 5400 e). This latest diamond has been measured in the laboratory in a characterisation station using a ^{90}Sr source. In Fig. 2 we show the pedestal subtracted pulse
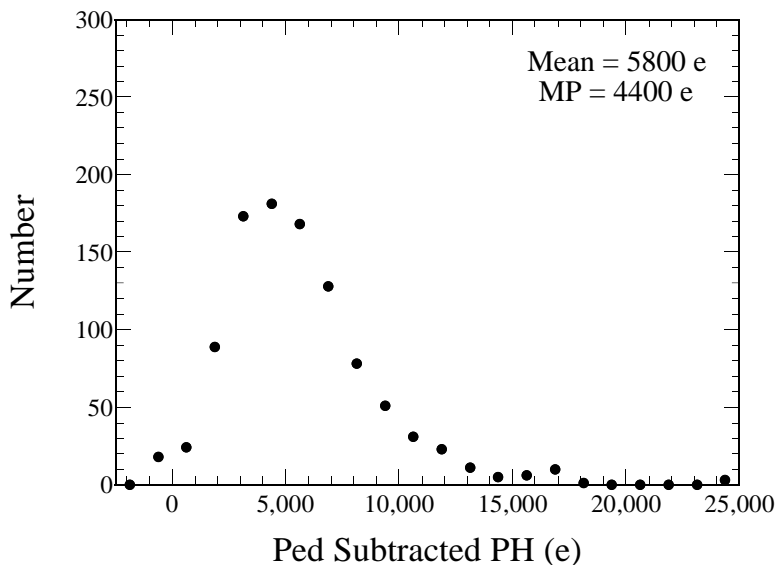

Figure 2: The measured pulse height at an electric field strength of 0.7 V/μm in one of the 1996 diamond samples after tuning the growth process and post processing the diamond.

height distribution of this diamond. The signal is Landau distributed with a mean to most probable ratio of 1.3. We obtained, in this run, from the mean charge of 5800 e a collection distance of 161 μm at an electric field strength of 0.7 V/μm. In subsequent runs we obtained a collection distance of 200 μm at an electric field strength of 0.9 V/μm. The small enhancement at zero pulse height is due to a false trigger contamination at the 3.6% level. We recently placed a 50 μm pitch strip detector on this diamond and tested it in a proton beam at CERN PS. The online results confirm the laboratory characterisation. The offline analysis is in progress and we expect results in the next few months.

The second important development involves an additional manufacturer. During the last year we have used diamond from two manufacturers: St. Gobain/Norton company [4] and DeBeers Industrial Diamond division [5]. Until recently, the highest quality CVD diamond was produced by St. Gobain/Norton. DeBeers has now produced CVD diamond with comparable and better collection distances.

2.1 How We Increased Charge Collection Distance

The basic method we have advocated with each company to increase the charge collection distances involves three parts: A serious chemistry study to understand the operating parameters of the different growth machines and their effect on the collection distance. For this part of the program we provide instantaneous feedback of the collection distance to the manufacturers. First we systematically measure charge collection distances. The collection distance is one of the most sensitive diagnostic parameters and we are able to use it to detect changes in the growth process in blind tests. Second the growth process is tuned and correlated to the collection distance measurements. The second part of the program involves the manufacturers producing a thick wafer, $\sim$ 700 μm, to understand the stability of the growth process and the thickness scaling laws for their diamond. The third step of the process includes post-growth treatment of the diamond in which the manufacturers remove up to 35% of the material from the substrate side

where the collection distance is nearly zero [3]; we then place the active pattern, strips or pixels, on the growth side of the diamond where the collection distance is largest. In Fig. 3 we show the results of material removal from one of the most recent diamonds. We see clear evidence that removing material from the substrate side improves the diamond collection distance. Also shown in Fig. 3 is the absolute prediction from a model where the collection distance increases linearly throughout the thickness of the material from zero at the substrate side to twice the bulk-averaged collection distance at the growth side. The data supports this simple model and confirms our earlier work which showed that the collection distance increases with material thickness [3]. We are well into this program. The program as outlined above takes 1 to 2 years for the manufacturer to reach the full potential of their individual process.
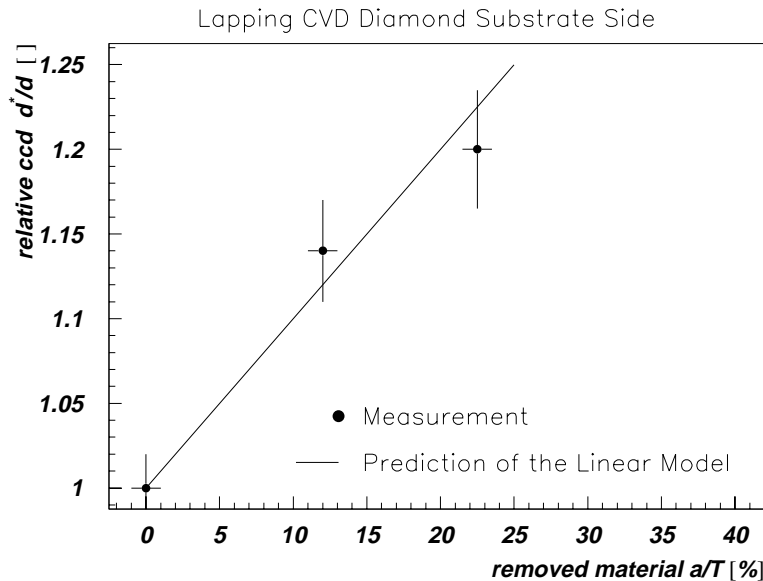

Figure 3: The scaled collection distance measured as a function of the percentage of material removed from the substrate side of the diamond.

2.2 What We Can Reasonably Expect in 1997

The program outlined above will lead to signal sizes of approximately 7000 e. A small amount of tuning will be required to reach signal sizes of 8000 e. This will take place in 1997 and 1998. Also during 1997 we propose to order 6 wafers of diamond which will provide enough of the new higher quality material to produce reasonably sized trackers and to complete the radiation hardness studies. Finally, in 1997 we will begin working with the manufacturers to determine how to reduce the production costs of the raw material. This stage will require additional chemistry experiments to assess the consequences, if any, for the collection distance as we change the growth conditions. Overall, at the end of 1997 we hope to have a working prototype of an LHC tracking element and realistic indications of the final cost of such a tracking element.

3 Irradiation Studies of CVD Diamond

Radiation hardness is required for particle detectors in future LHC experiments. In particular solid state tracking detectors have to resist high particle fluences keeping the signal-to-noise ratio as high as possible after irradiation.

Solid state devices are damaged under particle irradiation. Damage in solid state detectors causes on one hand an increase in leakage current and therefore an increase in noise; on the other hand a reduction in the amount of collected charge, which leads to a smaller signal. The signal-to-noise ratio in damaged detectors decreases. The potential advantage of diamond is the much larger dose that is apparently necessary to cause the same damage.
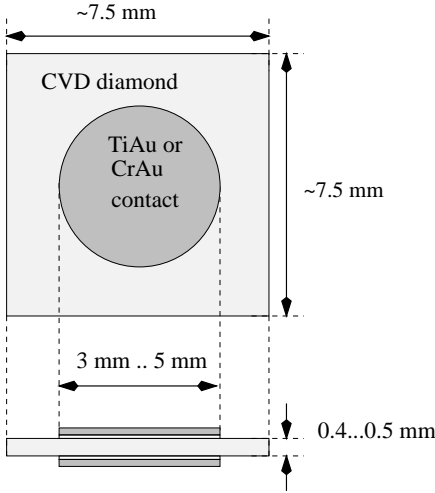
Figure 4: Geometry of a CVD diamond sample with round electrodes on both sides.
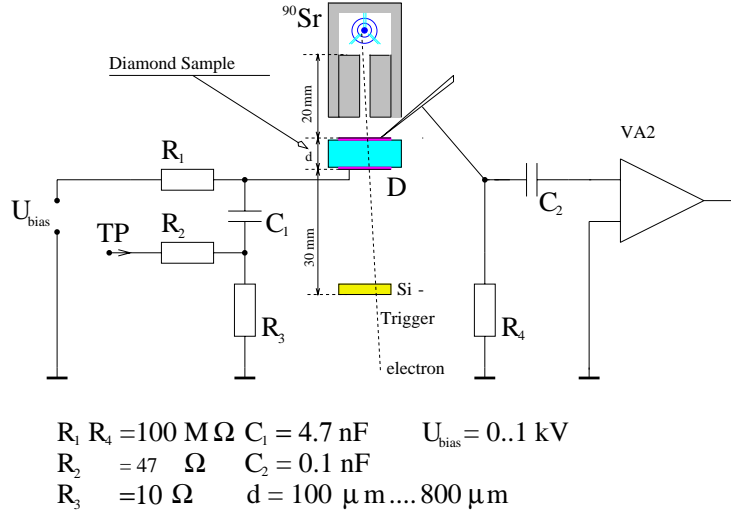
Figure 5: Setup for measuring charge collection distance on CVD diamond.

3.1 Method for Sample Characterisation

The radiation hardness was studied on CVD diamond detectors by measuring the collected charge and the leakage current before and after irradiation.

3.1.1 Dark Current

CVD diamond samples which were irradiated had a size is of 7.5×7.5 mm^2 and a thickness between 400 μm to 500 μm [Fig.4]. They were metallized with round electrodes forming ohmic contacts on both sides of the diamond. The *dark current* was measured as a function of voltage applied to the electrodes before and after irradiation in darkness.

3.1.2 Charge Collection Distance

The amount of collected charge is measured in a setup shown in Fig. 5. A voltage is applied to one side of the sample. The other side is connected to a charge integrating amplifier and shaper and is at a virtual ground. A ^{90}Sr electron source illuminates the sample. Electrons which traverse the sample trigger the readout of the amplifier. The amplitude of the shaped signal is proportional to the collected charge. In diamond the mean number of collected charges $\langle Q_{\mathrm{col}} \rangle$ is proportional to the *charge collection distance*, d_{c}, which is the mean distance charge

8

carriers travel apart inside the bulk before they are trapped [6], thus

$$d_{\rm c} = \frac{\langle Q_{\rm col} \rangle}{36 \ e/\mu{\rm m}}.$$ (1)

The charge collection distance is measured as a function of the applied voltage and, unless otherwise mentioned, we quote it at an electric field of 1 V/μm.

3.2   Photon, Electron and Proton Irradiations

It has been shown in the past that CVD diamond is resistant to electromagnetically interacting radiation.

In a photon irradiation in 1993 using a ^{60}Co gamma source at the Argonne National Laboratory CVD diamond samples were irradiated up to an absorbed dose of 10 MRad [7]. No decrease in charge collection distance was observed. In fact the opposite, a linear increase of charge collection distance between 0 and 1 kRad absorbed dose and a saturation above 10 kRad, was measured. The saturation value is known as the pumped state of the diamond, which is generally higher by a factor of 1.6-1.9 than the depumped state.

In an Electron Irradiation in 1995 at Société AERIAL with 2.2 MeV electrons from a Van de Graaf accelerator CVD diamond samples absorbed a dose of up to 100 MRad [8]. No decrease in charge collection distance was observed. As in the photon irradiation an increase of charge collection distance to the pumped value was measured.

Proton irradiations were performed on CVD diamond samples in 1994 and 1995 at TRIUMF, Vancouver, Canada using protons with a kinetic energy of 500 MeV reaching a fluence of 5×10^{13} $p/\rm cm^2$ at a maximum flux of 8×10^8 $p/\rm cm^2/s$ [9]. As in electron and gamma irradiations the charge collection distance increased to its pumped value. No decrease in charge collection distance was observed. Moreover a linear dependence between proton flux and induced current in diamond was measured.

3.3   Irradiation Studies in 1995 and 1996

During the last year a strong emphasis has been placed on irradiations of CVD diamond with pions and neutrons. Charged pions are the predominant source of radiation in LHC experiments. Unlike photons and electrons but similar to protons they will undergo nuclear interactions with the diamond, which might influence the charge collection distance differently than electromagnetic radiation. Neutrons will be present in any LHC experiment as well and their pure hadronic interaction damages the diamond lattice.

3.3.1   Pion Irradiations

CVD diamond detector samples were irradiated with pions in three separate exposures in 1994 [10], 1995 and 1996. All irradiations were performed at the PSI, Villingen, Switzerland. The pions had a momentum of 300 MeV/c. The maximum available pion flux onto the samples was $\mathcal{O}(1.5 \times 10^9)$ $\pi/\rm cm^2/s$. The samples had the same geometry as shown in Fig. 4. During irradiation the samples were biased with a voltage of 100 V or above. The total pion fluence on samples irradiated in 1994 and 1995 reached 5.6×10^{14} $\pi/\rm cm^2$.

The normalized charge collection distance measured on CVD diamond samples after irradiation with pions is shown as a function of pion fluence in Fig. 6. The charge collection distance is normalized to the depumped state of the sample before any irradiation. During characterisation with ^{90}Sr electrons the charge collection distance increases by a factor of 1.7. The samples remain in their pumped state after irradiation with pions and show no decrease of collections distance up to total pion fluences of 5.6×10^{14} $\pi/\rm cm^2$.

The dark current on these samples was measured before and after irradiation. A characteristic value is 0.5 pA/mm^2 at 1 V/μm. The dark current is independent of the received pion fluence. These measurements indicate that the detector performance was unchanged after irradiation up to 5.6×10^{14} π/cm^2.

The irradiation in 10/1996 increased the total fluence on the samples up to 1.7×10^{15} π/cm^2. In addition material from our new supplier was irradiated up to 1×10^{15} π/cm^2. The data from this run is presently being analyzed and should be available in the near future.
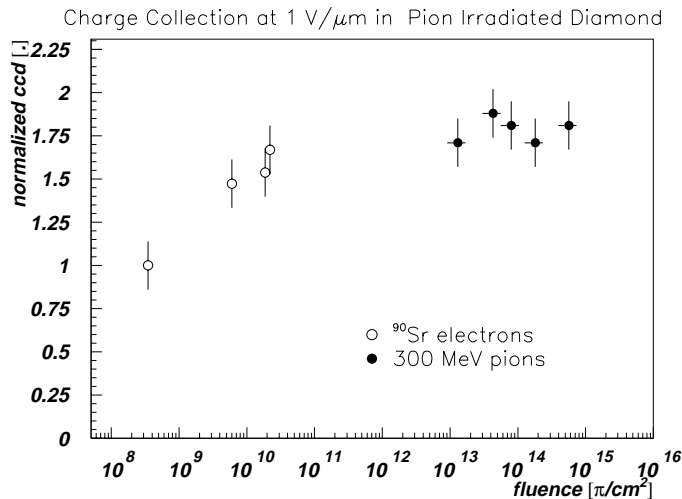

Figure 6: Normalized charge collection distance in diamond samples as a function of pion fluence.

3.3.2 Neutron Irradiations

CVD diamond samples and silicon diodes were irradiated with neutrons in four exposures (1/95, 10/95, 12/95 and 11/96). All irradiations took place at the ISIS facility at the Rutherford Appleton Laboratory, England. Neutrons with kinetic energies below 10 keV and energies peaking at 1 MeV were available [11]. The mean n-flux above 10 keV was about $(1.7 \pm 0.6) \times 10^8$ n/cm^2/s.

The diamond samples [Fig. 4] were irradiated at room temperature with a voltage of 100 V applied. The charge collection distance before neutron irradiation, after 3.2×10^{14} n/cm^2 and after about 1×10^{15} n/cm^2 is shown as a function of electron fluence in Fig. 7. The charge collection distance increases as a function of ^{90}Sr electron fluence from a depumped state and saturates at a pumped value. The pump-up factor of non-irradiated samples is 1.7. After irradiation with 3.2×10^{14} n/cm^2 the charge collection distance of the depumped value is lower than before irradiation, but it increases under ^{90}Sr illumination to a pumped value, which is equivalent to the pumped value before neutron irradiation. This result is confirmed by another set of samples which received 4×10^{14} n/cm^2. Hence there is no decrease in charge collection observed below 4×10^{14} n/cm^2.

After receiving 1×10^{15} n/cm^2 the charge collection distance of the depumped state decreases. Pumping with electrons increases the charge collection distance again, but a higher electron fluence is required. The charge collection distance saturates in a pumped state which is 15% lower than the pumped state of samples before neutron irradiation. A decrease in detector performance is therefore expected between 4×10^{14} and 1×10^{15} n/cm^2. Measurements of
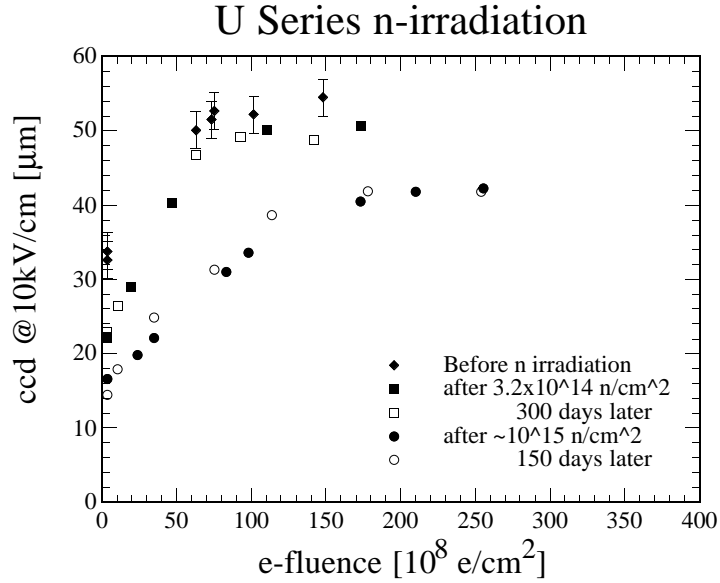
U Series n-irradiation

Figure 7: Charge collection distance of neutron irradiated diamond samples as a function of electron fluence before and after neutron irradiations.

several neutron irradiated samples were redone six months and one year after the irradiation and showed no change compared to the measurements immediately after the irradiation. Thus no annealing or anti-annealing effects are observed.

One sample accumulated a total fluence of 1.9×10^{15} n/cm^2 over three exposures. Its pumped value decreased by 25% relative to the pumped value before neutron irradiation. The normalized charge collection distance of the pumped state as a function of neutron fluence is shown in Fig.8.

The dark current was measured before and after neutron irradiation between -1 V/μm and +1 V/μm on depumped samples. No change in dark current was observed up to 1.9×10^{15} n/cm^2.
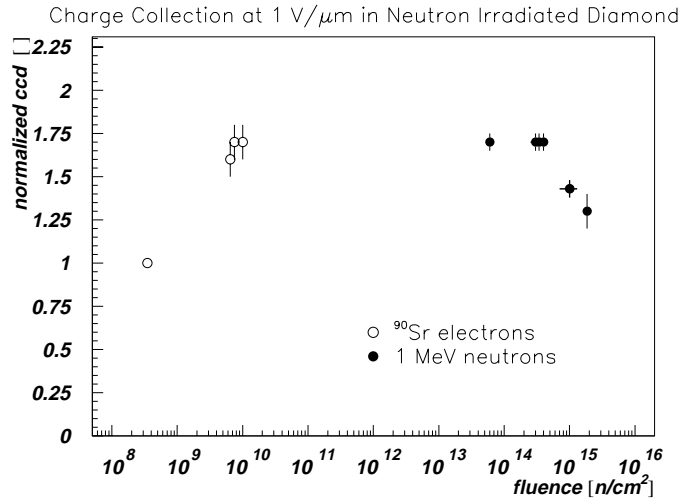

Figure 8: Normalized charge collection distance of diamond samples as a function of neutron fluence.

During the most recent irradiation the beam induced currents in the diamond detectors and the silicon diodes were recorded every 5 minutes. Figure 9 shows the currents from a silicon diode and a diamond sample as a function of time during the irradiation. Both samples have

the same electrode size. The current in diamond is several hundred pA when the beam is on. It stays roughly constant over the 120 hour time interval shown. The induced current in diamond decreases by a factor of 100 during beam-off periods. The diamond sample shows a prompt response when beam returns. This is most likely due to the presence of photons associated with the neutron beam. The behaviour of the diamond is nicely contrasted by the current in the silicon diode which shows a linear increase from 100 pA to 30 μA after 120 hours. During beam-off periods the silicon current decreases due to annealing.
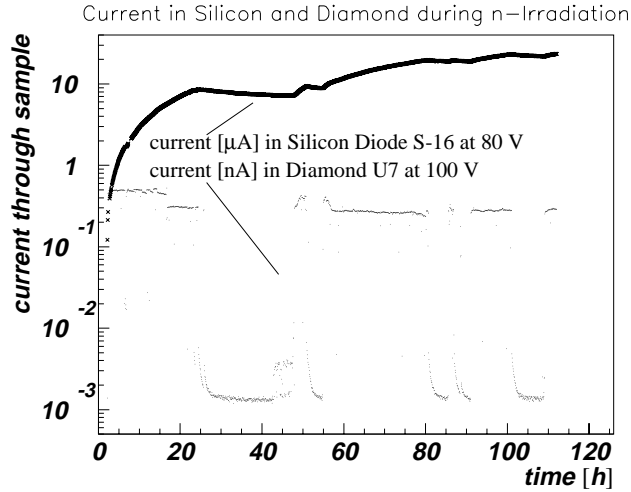

Figure 9: Currents in a silicon diode and a diamond sample during neutron irradiation.

3.4   Conclusion on Irradiation Studies

CVD diamond samples were exposed to pions and neutrons in serveral irradiations over the last two years. After pion irradiation no degradation in charge collection up to 5.6×10^{14} π/cm^2 is observed. The leakage current after pion irradiation is the same as before irradiation. After neutron irradiation no degradation up to 4.0×10^{14} n/cm^2 is observed. The charge collection distance decreases by $\approx 15\%$ between 0.4 and 1.0×10^{15} n/cm^2 and by $\approx 25\%$ by 1.9×10^{15} n/cm^2. The leakage current remains unchanged even after 1.9×10^{15} n/cm^2.

We conclude that diamond is a radiation hard detector material which is able to withstand the conditions in high particle fluence regions of detectors at the LHC.

4   Results from Diamond Tracking Detectors with Slow Electronics

In 1995 and 1996 a series of beam tests performed at CERN explored various aspects of the performance of tracking detectors made from CVD diamond. These included tests of 50 μm pitch, 1 cm $\times$ 1 cm, single-sided detectors using the VA2 readout chip with 2 μs shaping, tests of the same detectors in a magnetic field and the first test of a diamond pixel device.

4.1   Recent Work on Strip Detectors with Slow Electronics

The VA2 chip allows for ultra-low noise levels of 100 electrons ENC with a shaping time of 2 μs due to the negligible leakage current in CVD diamond. Though clearly not useful in a high luminosity environment, this allows one to study detectors thoroughly in a test beam.

Using the 100 GeV/c pion beam in the X5 West Area at CERN we studied trackers made from various diamond samples. All the devices were metallized with a solid electrode on one side, and 50 μm pitch strips on the other. The strips were wire-bonded to a VA2 chip, and the detectors mounted in a telescope with eight silicon planes (four x and four y). The arrangement appears schematically in Fig. 10. The hit resolution and geometry of the detectors allows an accuracy of better than 3 μm in projecting a track into a test detector plane after alignment.

All data were pedestal subtracted, and corrected for common-mode fluctuations which were typically much smaller than the individual channel noise. Clusters were found by seeking the maximum pulse height strip in a plane, and adding to it any adjacent strips with pulse height more than 2σ above zero. Events in which the track extrapolates to non-functioning regions of the detector were not considered.
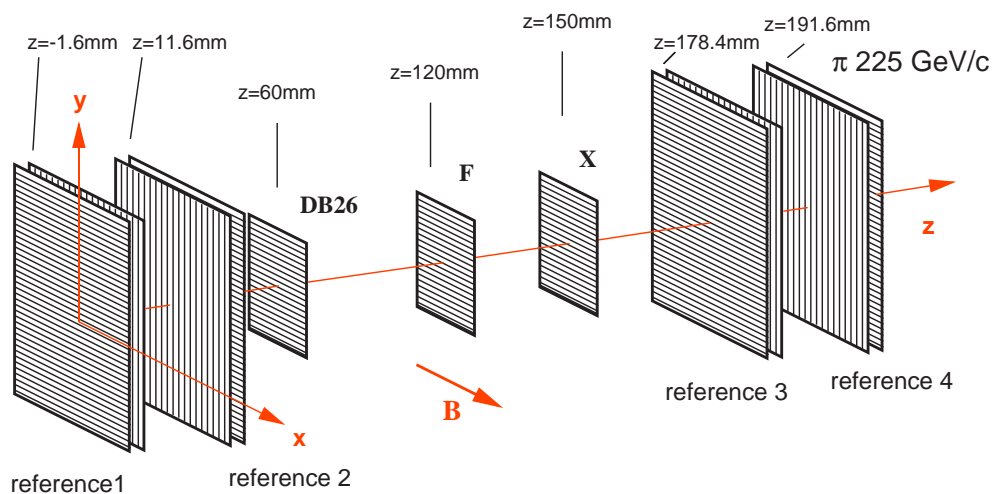

Figure 10: Setup of the silicon telescope with diamond detectors in the test beam.
For the the magnetic field test the magnetic field lines are parallel to the x coordinate.

Until recently our best diamond was the F detector. The results from this diamond with strips on the substrate side were reported in the 1995 RD42 Addendum [2]. Its pulseheight distribution is shown in Fig. 11. The cluster pulse height distribution of the F detector in a recent run is shown in Fig. 12. The F diamond has a collection distance of approximately 100 μm. The resolution obtained is shown in Fig. 13. These results are comparable with those reported last year indicating the stability of this detector. The observed resolution of 13.4 μm, only slightly better than digital resolution, is quite typical of the resolutions we have observed during the past year. That the resolution is only slightly better than digital resolution indicates that we do not observe much charge sharing. Inspection of individual cluster shapes, a representative
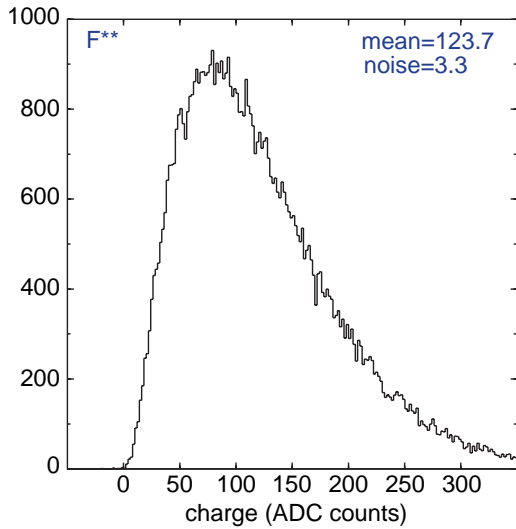
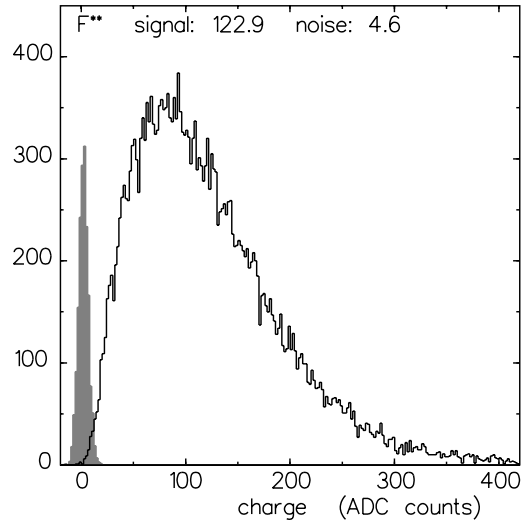Figure 11: Pulse height distribution measured on F in July 1995.

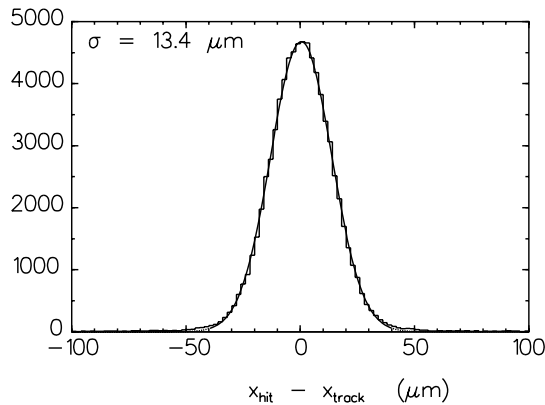Figure 12: Pulse height distribution from the F detector with a 50 μm pitch strip detector.

Figure 13: Hit position resolution in the F detector.

sample of which appears in Fig. 14, reveals that while the strip through which the track passes has a large, positive pulse height, adjacent strips on both sides tend to have negative pulse height.

After observing the cluster shapes in the F diamond a series of tests was made with the X detector. The purpose of these tests was to compare the signal shapes in strip detectors with the strips on the growth versus substrate side. The X detector was polished on the growth side so that in successive beam tests the strips could be put on the growth and then the substrate side.

As shown in Fig. 15 and Fig. 16, with strips on the growth side the clusters are narrow having a one or two strip central peak and the adjacent strips are negative. With strips on the substrate side the clusters are broad, covering many strips. In both cases the adjacent strips go negative, consistent with our understanding of the charge transport mechanisms at work.

We propose a simple model to explain the effects we see. After the passage of a charged particle the electron-hole pairs move under the influence of the applied electric field. For each electron-hole pair one carrier moves toward the strips, and the opposite-sign carrier moves away from the strips. Hence any non-uniformity in the material will cause the spatial extent of the induced charge to depend on the carrier sign. The fact that the collection distance depends

14
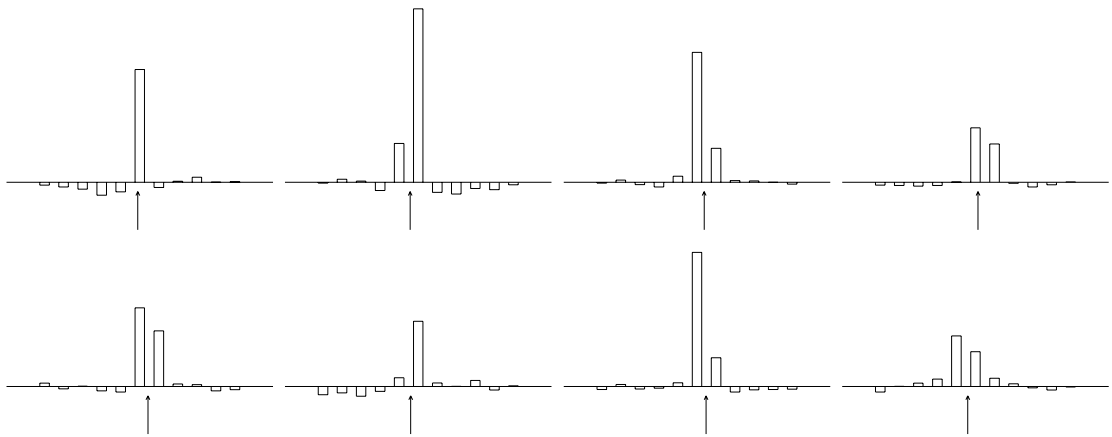
Figure 14: Typical cluster shapes in the F detector. The arrow indicated the predicted track position from the silicon telescope.

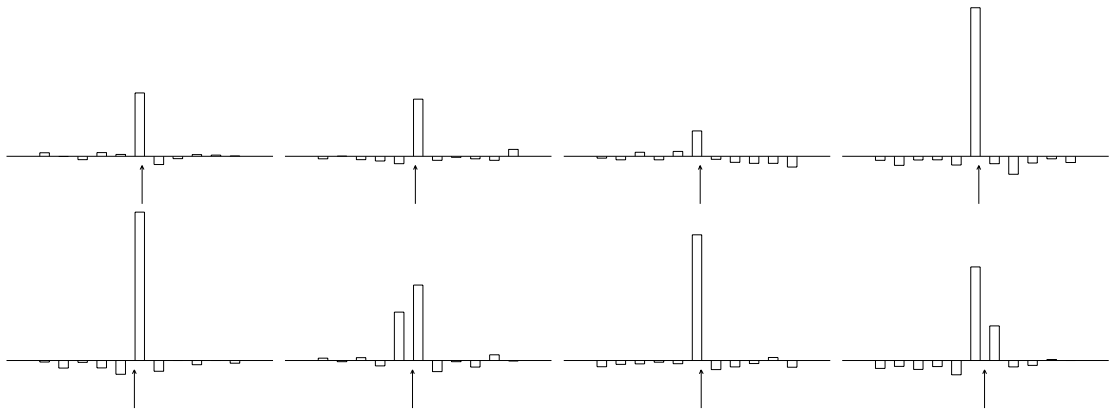Figure 15: Typical cluster shapes in the X detector with strips on the growth side. The arrow indicates the predicted track position from the silicon telescope.
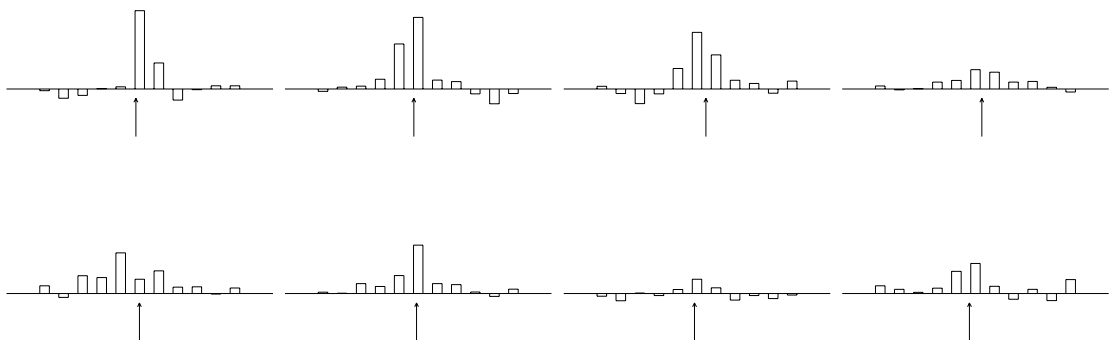
Figure 16: Typical cluster shapes in the X detector with strips on the substrate side. The arrow indicates the predicted track position from the silicon telescope.

on depth into the material causes just such a spatial non-uniformity and complicates matters. Whereas the total charge observed must be equal on the two sides of a detector, the shapes will differ depending on the distance between the moving charge and the readout strips. Generally speaking, one would expect that for a detector with strips on the substrate side (low collection distance side), the cluster shapes should be broader, since most of the charge motion is far from the strips. Conversely, for strips on the growth side (high collection distance side), the cluster shapes should be narrow since most of the charge motion is near the strips. Since the electronic noise sets an effective threshold, below which charge is unobserved, in general we will be able to cluster a larger signal when the strips are on the growth side.

We have presently lapped the growth side of the F diamond, placed a 50 μm strip detector on the growth side and are in the process of analyzing the testbeam data to complete these studies.

4.2 Diamond Pixel Detectors

In August 1996 the first diamond-based pixel tracking detector was tested. This detector was read out with a VA3 chip wire bonded to a pixel fanout structure metallized on a glass substrate. The 16×16 array of pixels, having 150 μm^2 pitch, was bonded to pixels metallized on the diamond using a technique in which 20 μm diameter wires were affixed, using conductive glue, to the pixels on the diamond, and cut to a length of 60 μm. The structure is dipped into conductive glue, coating the tips of the wires, and then placed in contact with the readout pixel array [Fig. 1].
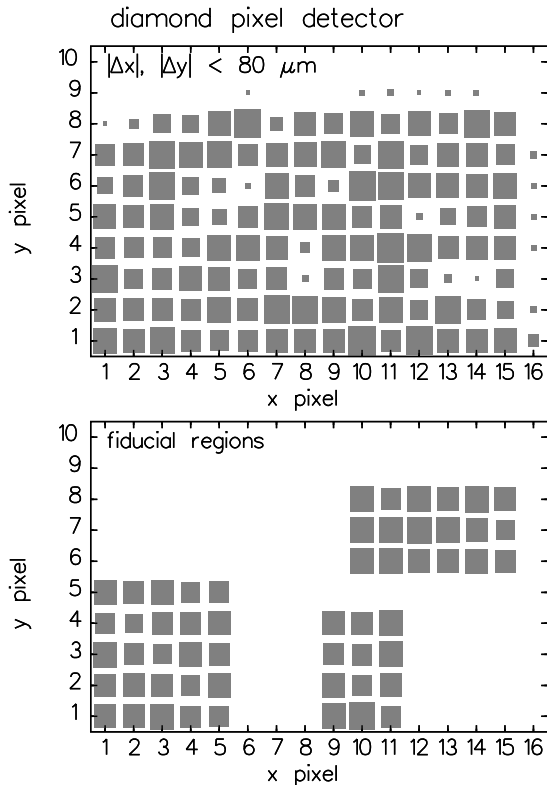

Figure 17: Determination of fiducial region of pixel detector. Top plot shows number of tracks in each pixel giving cluster position within 80 μm in x and y of the track. Bottom plot shows retained region after fiducial cuts.

In the beam test, only 128 channels were read out, and thus only one half of the array was

tested. To analyze the data we first find a single 2D cluster in the array by starting with the pixel with largest pulse height, and add to it any of the eight adjacent pixels whose pulse height exceeds zero by at least twice the single channel noise. The cluster position in two dimensions comes from the weighted average in each dimension. One can then align the detector by comparing the cluster positions with the extrapolated track position. An accuracy of roughly 10 μm is attained.

A fiducial region, determined by plotting the track position for those clusters within 80 μm of the track, covers three sub-regions of the detector. Figure 17 shows, for each pixel, the number of tracks which gave a cluster centered on that pixel having a centroid within 80 μm of the track position. The reconstructed clusters uniformly populate the detector Fiducial cuts are applied to remove the "holes" near the locations of unbonded pixels.

The detector has a position resolution of just under 50 μm in each dimension. Figure 18 shows the two-dimensional distribution of the difference between the cluster and track position, and Fig. 19 shows the individual coordinate projections with Gaussian fits.
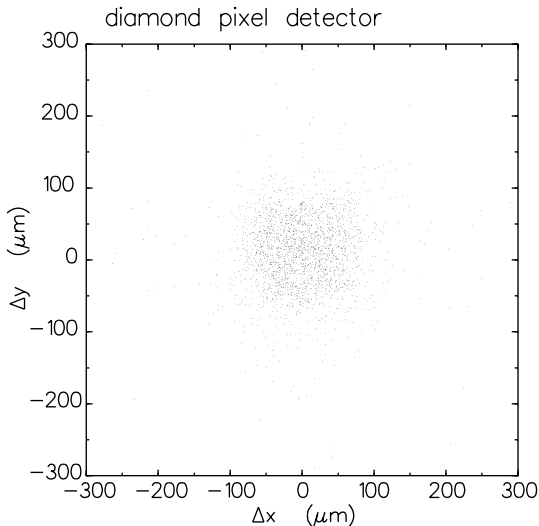
Figure 18: Two-dimensional distribution of difference of pixel cluster position and track position.
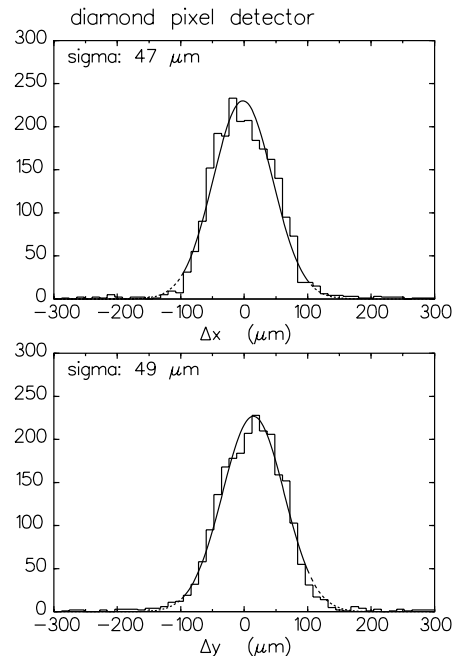
Figure 19: Individual x and y resolution distributions for the diamond pixel detector.

To estimate the charge collection of the pixel detector one can perform a transparent analysis by adding the total charge in the nine pixels surrounding the extrapolated track position. Figure 20 shows this distribution, which has a collection distance of 45 μm. The individual channel noise was 75 electrons on average. This is the first demonstration of the operation of a diamond pixel detector.

4.3   Diamond Strip Detectors in a Magnetic Field

Diamond strip detectors based on CVD diamond material have been studied at high magnetic field. The detectors were tested in a 225 GeV/c pion beam at the CERN SPS accelerator. The diamond detectors F and X, had 6.8 mm long strips with a pitch of 50 μm on one side and a
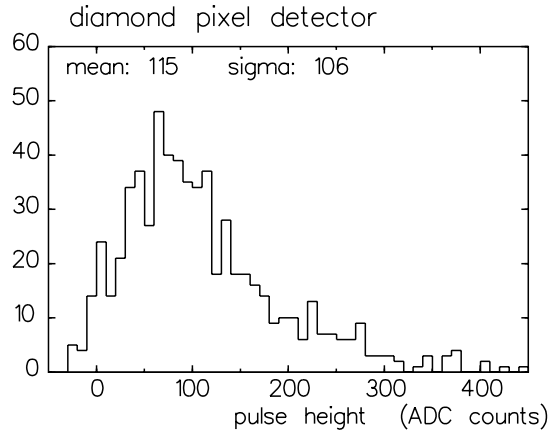
Figure 20: Nine pixel pulse height distribution in fiducial region of the diamond
pixel detector.

continuous contact on the other side. Each strip was read out by a VA2 amplifier chip with an
integration time of 2 μs.

The diamond detectors were placed in the center of a reference telescope consisting of 4
planes of silicon strip detectors measuring the track coordinates in the plane perpendicular to
the beam, x and y. The reference system and test detectors were located in the center of a
superconducting magnet providing a field of up to 3 T along the horizontal x coordinate. The
strip orientation of the diamond detectors was parallel to the magnetic field. All detector planes
were perpendicular to the beam axis. Figure 10 shows a schematic illustration of the test setup.

4.3.1   Reference System and Event Selection

The reference system was aligned using data taken at $B = 0$. The diamond detectors, which
were not used in the track fit, were aligned with respect to the reference system. These alignment
parameters were subsequently used for the analysis of all data taken at magnetic fields of 0, 2
and 3 T.

Figure 21: Track slope and residual distribution in the reference silicon detectors shown for
one of the silicon planes.

Events were selected requiring exactly one track measured in both coordinates of all reference
planes. Tracks were reconstructed as straight lines. Events with noise hits and multiple tracks

18

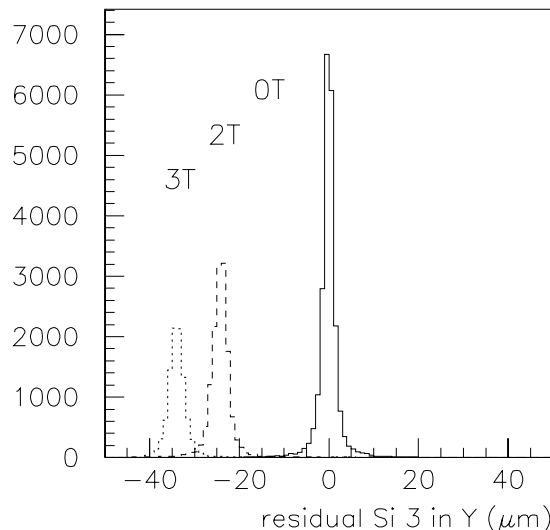were rejected. Clusters were defined as a sequence of adjacent strips with a S/N ratio higher than 1.5. Only clusters with a total S/N higher than 5 were accepted. Note that the same cluster definitions were used both for diamond and silicon detectors. Clusters containing noisy strips were rejected. Diamonds were required to have exactly one cluster in order to be considered in the analysis.

The magnetic field causes the particle track exiting the telescope to slope by 4 and 6 mrad at fields of 2 and 3 T respectively. Figure 21 shows the residual distribution for the silicon reference plane 3 measuring the y coordinate. The Lorentz shift of the clusters is visible. The sign of the shift depends on the orientation of the electric field depleting the silicon plane and is different in alternate y planes.

4.3.2   Diamond Cluster Parameters at Different Fields

The clusters on the diamond detectors were reconstructed and required to be in a 0.5 mm region on either side of the predicted hit position. Events with tracks outside the diamond's acceptance were rejected. The signals, measured by an ADC, were calibrated with pulses on a test capacitance, yielding calibration constants of 31.0 e/ADC count for diamond X and 26.6 e/ADC counts for diamond F. At the time of the measurements diamond F was in a pumped state, diamond X in a depumped state.
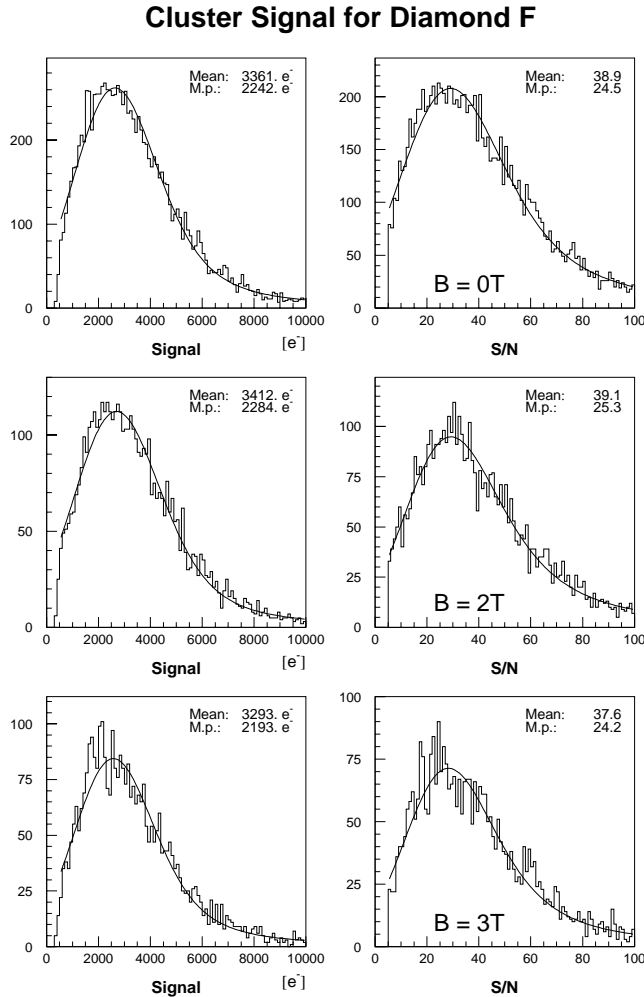
Cluster Signal for Diamond F

Figure 22: Cluster signal and S/N at different values of the magnetic field for diamond F

diamond detector	F			X		
magnetic field [T]	0.0	2.0	3.0	0.0	2.0	3.0
mean signal [e]	3361.	3412.	3293.	1612.	1580.	1522.
most probable signal [e]	2242.	2284.	2193.	794.	756.	758.

Table 1: Mean and most probable signal in electrons for diamonds F and X at different values of the magnetic field.

The signal distribution of diamond F, as shown in Fig. 22, remained essentially unchanged at all magnetic field values. The mean signal was about 3400 electrons, which corresponds to a collection distance of 94 μm. The signal was contained in two strips on average. The uniformity of the signal over the diamond area has been verified. No regions of low signal were observed. Signal parameters for both diamonds are summarized in Table 1.

4.3.3 Spatial Resolution, Signal Shape and Lorentz Shift

Tracks were reconstructed as straight lines between reference planes 1—4. The Lorentz shifts in the reference detectors were not taken into account. Since they had opposite signs in planes 1 and 2 with respect to planes 3 and 4, and since the track slopes were small, reconstructed tracks were not systematically shifted in the reconstruction from their true position. Only the sagitta between the real, curved particle trajectory and the reconstructed straight line had to be taken into account. The bending radius R (in m) can be calculated as

$$R = 3.33 \frac{p}{Bq} \tag{2}$$

where p denotes the particle momentum transverse to the B-field (in GeV/c), B, the magnetic field (in T) and q, the charge of the particle in units of the elementary charge. This yields a bending radius of 250 m for B=3 T and 375 m for B=2 T. The sagitta, s, between the real track and the reconstructed line is approximately

$$s = \frac{dz(L - dz)}{2R} \tag{3}$$

where L=180 mm is the distance between the two sets of reference planes and dz the distance of the diamond detector to the first reference plane (see Fig. 10).

The Lorentz shift of the clusters Δy in the diamond detectors can be obtained from the calculated sagitta plus the measured shift of the residual distribution with respect to the reconstructed straight line. Alternatively the position of the maximum signal can be measured with respect to the predicted hit position when the hit extrapolation is displaced by the expected sagitta. Both methods were used to determine the Lorentz shift of the clusters.

Figure 23 shows the residual distribution of diamond F for fields of 0, 2, and 3 T. The resolution of 15.8 μm is found to be constant within the measurement uncertainty. A clear shift of the residuals at 2 and 3 T is visible. The measured Lorentz shift, after correction for the sagitta, is 24.8 μm at 3 T and shows a linear dependence on the magnetic field.

Diamond X exhibits a slightly worse resolution of 17.9 μm than diamond F, but no significant change with magnetic field. The Lorentz shift is 18.1 μm at 3 T with the same type of dependence as for diamond F. The size of the two shifts has been understood in terms of the relative thickness of the two samples.

In the second analysis the signal shape and position were investigated at different values of the magnetic field. For this analysis the average signal of a single strip was plotted versus the predicted track position with respect to the strip center. This allows a study of the spread of the
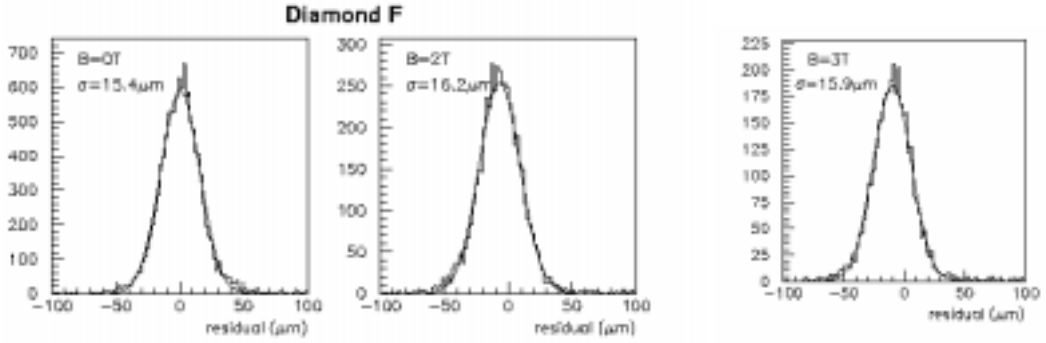
20

Figure 23: Residual distribution for diamond F at different magnetic field strengths.

signal under the influence of diffusion and the magnetic field. A shift of the charge cloud result from the Lorentz force which could introduce an asymmetry of the measured charge cloud. As this analysis uses only the predicted hit position it is independent of cluster thresholds.
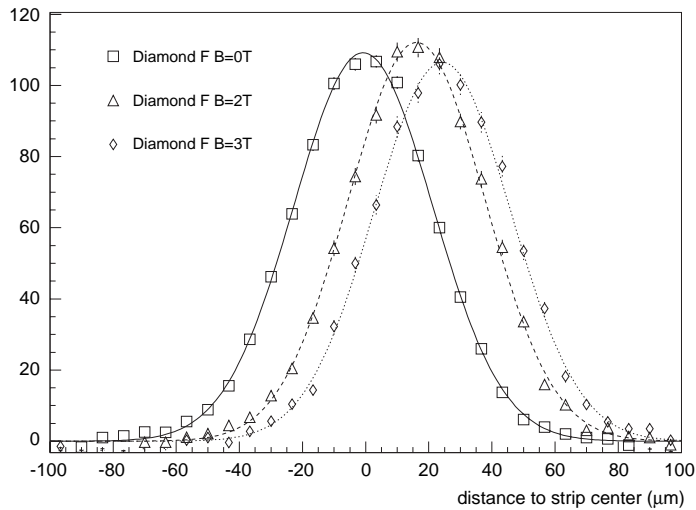
Figure 24: Signal shape for different values of magnetic field strength in diamond F.

Figure 24 shows the average strip signal versus the predicted hit position. The predicted hit position is calculated from the track extrapolation and the sagitta. The plot gives the signal shape as projected on the plane perpendicular to the strips for diamond F at fields of 0, 2 and 3 T. The measured points are fitted to a Gaussian distribution. It can be seen that both the size and the shape of the signal remain unchanged with the magnetic field. The width of the distribution, as given by the σ of the Gaussian fit, is 22 μm. No asymmetry of the signal shape with respect to its center is observed. The Lorentz shifts are consistent with those measured in the first analysis. Also for diamond X the shift of the cluster as a result of the Lorentz force increases with the magnetic field. No significant asymmetry beyond the statistical errors is observed. With a width of σ=35 μm clusters measured on diamond X are substantially wider than on diamond F, but do not change with the magnetic field.

Using this data we may also deduce the mean Lorentz angle $\langle \alpha \rangle$ throughout the diamond. We use the term *mean Lorentz angle* since the collection distance is not constant through the detector. If we define t as the thickness of the material, and $\langle \Delta y \rangle$ as the average shift of our

diamond detector	F			X		
magnetic field [T]	0.0	2.0	3.0	0.0	2.0	3.0
Resolution [μm]	15.4	16.2	15.9	17.8	18.3	17.5
Sagitta [μm]	0.0	10.0	15.0	0.0	6.8	10.2
Δy from residuals [μm]	0.0	16.7	24.8	0.0	12.1	18.1
Δy from charge distribution [μm]	0.0	16.2	24.3	0.0	12.5	17.3
$\langle\alpha\rangle$ [degrees]	0.0	4.6	6.8	0.0	4.5	6.5

Table 2: Resolution, sagitta of the track, Lorentz shift, and Lorentz angles for diamonds F and X at different values of the magnetic field. The Lorentz shifts have been calculated using two different methods (see text). The Lorentz angles were calculated using the average Lorentz shift.

two measurements then the mean Lorentz angle is given by:

$$\tan(\langle\alpha\rangle) = 2 \times \langle\Delta\text{y}\rangle/t \qquad (4)$$

Resolutions and Lorentz shifts and Lorentz angles for both diamonds and for all values of the magnetic field are shown in Table 2.

4.3.4   Summary on Diamond Trackers in a Magnetic Field

The influence of a magnetic field on signal and spatial resolution of diamond strip detectors has been studied. The magnetic field causes a shift of the clusters, which increases linearly with the magnetic field strength, but does not change spatial resolution, cluster signal or width. The Lorentz shift is found to be different for diamonds F and X, but the Lorentz angle, relating the shifts to the respective detector thicknesses is the same. Fig. 25 shows various detector parameters of diamonds F and X versus the magnetic field strength.
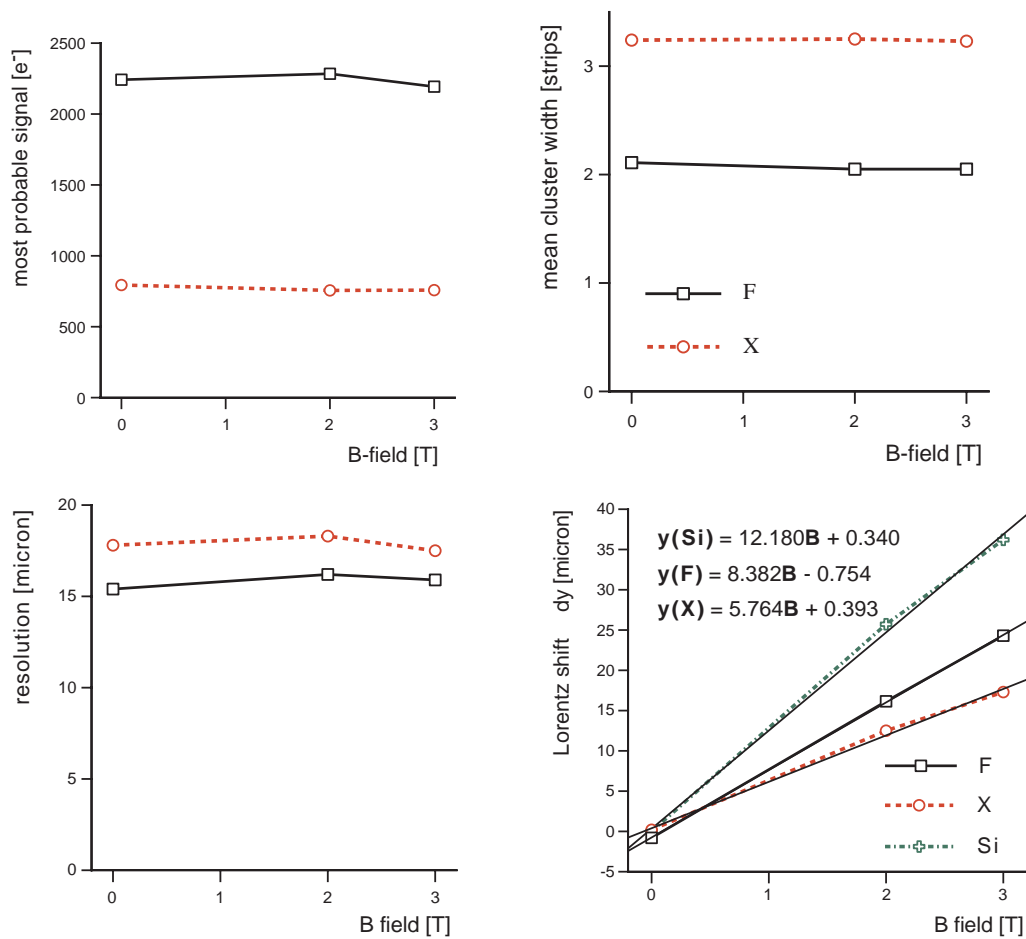
Figure 25: Mean cluster signal (top left), cluster width (top right, in units of readout pitch), spatial resolution (bottom left) and Lorentz shift (bottom right) at different values of the magnetic field. The Lorentz shift as measured on silicon strip detector reference Y3 is compared to the diamond data.

5 Diamond Detector with LHC Speed Radiation Hard Readout

An important step towards the use of CVD diamond detectors in an LHC experiment is the demonstration of their tracking capability using fast and radiation hard LHC readout electronics. In the following a first attempt to use such electronics for the readout of a diamond strip detector is described. First results with existing electronics from lab and beam tests are shown. A discussion of a possible optimisation of this front end electronics for readout of diamond detectors is presented.

5.1 Diamond Detector with Existing Fast Electronics for Silicon Detectors

5.1.1 The Front End Chip: SCT32A

The front end chip used was the 32-channel SCT32A [12] which has been developed for readout of the ATLAS SCT Silicon strip detectors. Each channel of this chip consists of a bipolar preamplifier shaper input stage followed by a 112 cell analog pipeline and a 32-channel output multiplexer. The shaper provides a signal with a peaking time of 21 to 25 ns depending on the capacitive load. The analog pipeline samples the output of the shaper at 40 MHz clock frequency. The output multiplexer in this version can run up to a speed of 20 MHz. The chip is produced in radiation hard DMILL [13] technology.

5.1.2 Testbeam Setup

The diamond strip detector, Norton diamond F, used in this test has an area of 6.8×6.8 mm^2 with 25 μm wide strips at a pitch of 50 μm. Two adjacent strips were connected to one readout channel of the SCT32A chip. Hence the effective readout pitch was 100 μm. Prior to the beam test the detector was pumped with a ^{90}Sr source for 17 hours. The test was performed in the CERN SPS X5 test beam with 100 GeV/c pions.

We used the same silicon reference system as in the tests described previously shown in Fig. 10. The diamond detector was placed in the center of the telescope during the tests. The readout of the diamond detector was controlled by a sequencer which supplied the control signals to the SCT chip. After receiving a trigger from the scintillators a signal T1 was sent to the SCT chip to mark the pipeline cell corresponding to the triggertime for readout. The T1 signal and the scintillator trigger times were recorded with a TDC (100 ps/TDC count). The timing information was later used in the analysis to determine the precise delay between T1 and the trigger signal.

In the analysis events were selected by requiring one and only one track measured in both co-ordinates of all reference planes. The particle track was reconstructed as a straight line and a track extrapolation was made to the diamond detector.

5.1.3 Cluster Analysis

Prior to the cluster search the raw data were corrected for the channel pedestal and common mode shifts. This yielded a Gaussian noise distribution with a standard deviation of 660 electrons for a single channel. A calibration constant of 138 electrons per ADC count was determined by laboratory measurements of the chip noise. A cluster on the diamond is defined as sequence of strips with a signal to noise ratio S/N higher than 1.0. Clusters were accepted in the analysis if the total cluster S/N was higher than 2.5 and the cluster was located in a 0.3 mm wide region around the predicted hit position. The cluster position was reconstructed with the η-algorithm.

Using the TDC data a time window was determined, where the T1 signal was recorded in a 12 ns wide region around the peaking time of the amplifier [Sec. 5.1.4]. Events with a hold time in this window are accepted for the cluster analysis.
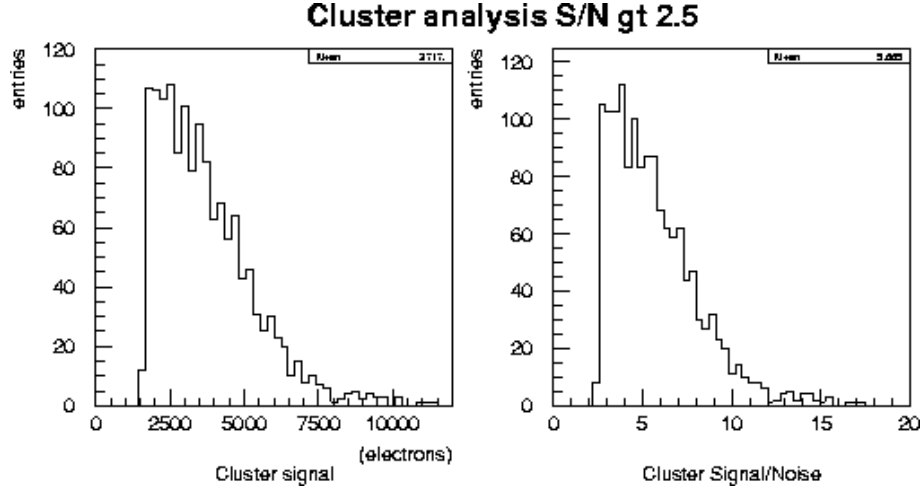
Figure 26: Cluster signal distribution and signal to noise distribution obtained in the cluster analysis with a S/N threshold of 2.5 on diamond F with SCT32A readout.

Figure 26 shows the cluster signal distribution and the cluster S/N distribution for the diamond. A mean signal of 3700 electrons and a mean S/N of 5.7 was measured. Both values are biased towards higher signal, or S/N, due to the threshold on the cluster S/N. Figure 27 shows the residual of measured minus predicted hit position for the diamond. The measured spatial resolution of 36 μm is close to the digital resolution of readout pitch divided by $\sqrt{12}$.
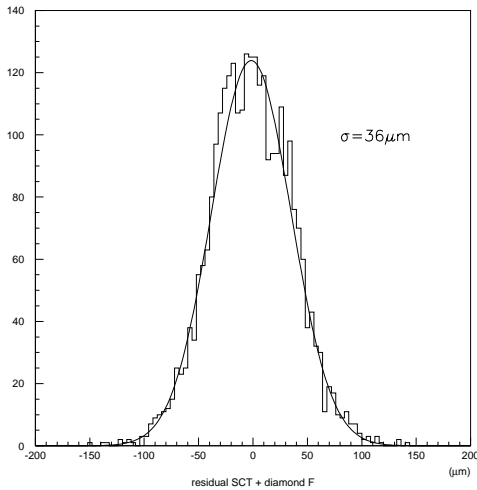
Figure 27: Residual distribution on diamond F with SCT32A readout.
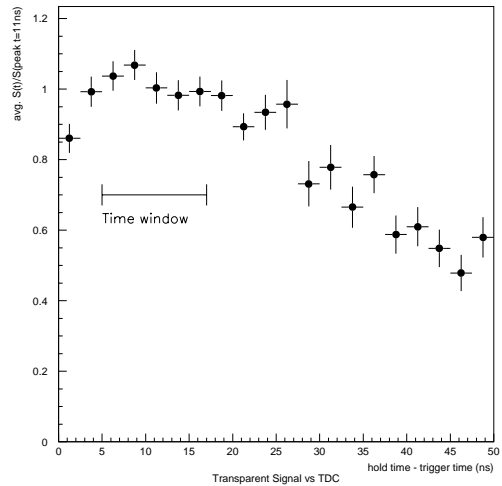
Figure 28: Transparent signal on three strips versus time difference of hold and trigger signal

In the cluster analysis with a threshold of 2.5 on the cluster signal to noise the efficiency is determined to be 67%. Previous test beam measurements indicated an efficiency higher than 90% for this diamond [14]. Two effects are thought to contribute: Firstly, the T1 signal was not sent in time to the SCT chip for some events, thus the signal was not measured. Secondly, the cut on the cluster S/N removes events with small signals from the analysis. To cross-check the latter hypothesis a transparent signal analysis was carried out on this data.

5.1.4   Transparent Signal Analysis

In order to obtain an unbiased estimate of the diamond signal, only the hit prediction is used in the signal search. No cut is applied to the number of clusters found on the diamond or diamond signal. The so-called transparent signal is calculated as the signal sum of three strips closest to the predicted hit position. In this way small signals are included in the analysis.

Figure 28 shows the average transparent signal versus the time difference between T1 and trigger signal. The average signal is normalized to the average peak signal. The plot indicates the time window used in the full analysis. A clear decrease of signal is observed for events where the T1 signal arrives before or after the peaking time of the amplifier. Figure 29 shows the transparent signal on three strips for events in the time window (markers). A Landau distribution convoluted with a Gaussian ($\sigma_{fit} = \sqrt{3}\sigma_{noise}$) is fitted to the transparent signal. This yields a peak transparent signal of 2300 e, equivalent to a S/N of 3.5, and a mean signal of 2843 e, corresponding to a mean S/N of 4.3. Previous measurements of this diamond with slow VA2 electronics yielded a most probable signal of 2240 electrons [14]. The comparison shows that there is no change in the collected signal due to the fast shaping time. Using previous signal measurements of this diamond and the noise obtained for the SCT one expects a peak S/N comparable to the measured S/N. As a dashed line the cluster signal obtained with a S/N threshold of 2.5 is superimposed. The difference for small signals suggests that the S/N threshold removes some fraction of the signal distribution and hence contributes to the inefficiency.
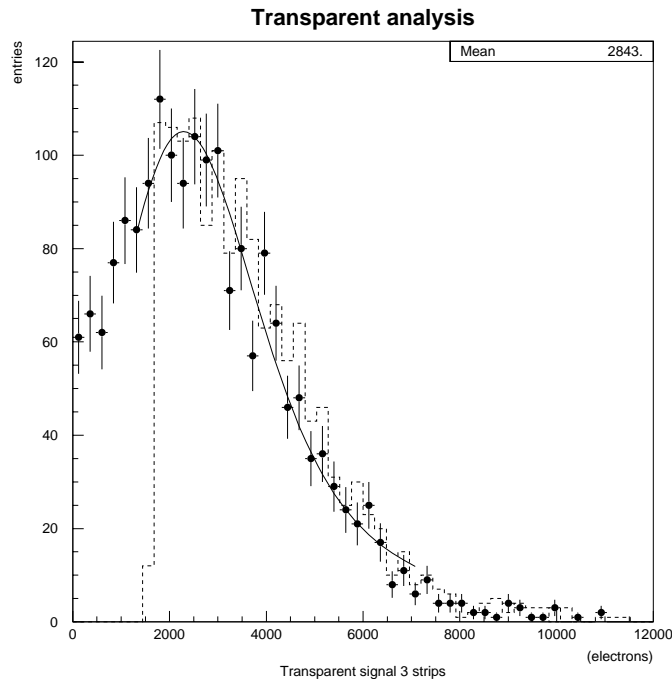
Figure 29:   Transparent signal on three strips (markers) fitted by a Landau distribution convoluted with a Gaussian distribution (solid line). The cluster signal obtained with a S/N threshold of 2.5 is superimposed as a dashed line.

5.2   Expected Performance of a Fast Readout Chip optimized for Diamond Detectors

The results presented in Fig. 29 have been obtained with a readout chip designed for use with silicon strip detectors in the ATLAS silicon tracker with a typical load capacitance of 20 to 25 pF.

To optimise the performance for CVD diamond strip detectors the input circuit of this chip must be modified. Two modifications are necessary. The feedback resistor value of the preamplifier has to be raised and the gain of the first stage has to be increased by approximately a factor 3 to eliminate noise contributions from the later stages which now give a sizeable contribution to the overall noise at low capacitances. The noise contribution from later stages is at present about 400 electrons ENC.

For diamond strip detectors with 6 cm long strips and 50 μm pitch one expects a load capacitance, C_d, of 4 to 5 pF. For such low capacitances the noise in the present chip is dominated by the parallel noise from the preamplifier feedback resistor R_f, which is laid out with R_f=100 kΩ. This gives a negligible parallel noise contribution when used with silicon strip detectors. The equivalent noise charge due to parallel or current noise is $\text{ENC}_p = F_i i_n \sqrt{T_p}$, with F_i a constant for a given transfer function of the shaper, T_p the peaking time in the shaper and i_n the square root of the current noise power density. The current noise power density is given by $i_n = \sqrt{2qI_{eq}}$ with $I_{eq} = I_b + I_d + 2kT/(qR_f)$ where I_b is the base current of the input bipolar junction transistor (BJT) and I_d is the detector leakage current. The term $2kT/(qR_f)$ is the equivalent in terms of noise current for the feedback resistor and is equal to 500 nA for $R_f = 100$ kΩ.

The detector leakage current, I_d, is negligible in case of diamond detectors. With a bipolar input transistor in the preamplifier, the irreducible minimum noise, which can be achieved, is determined by the optimal choice of the collector current I_c to balance the parallel noise from the base current I_b and the series noise $\text{ENC}_s = F_v v_n C_{in}/\sqrt{T_p}$ generated by the input transistor. In this expression the voltage noise power density v_n^2 depends on the collector current through

$$v_n^2 = 4kT \left(r_b + \frac{kT}{2qI_c} \right). \tag{5}$$

where r_b is the base spread resistance of the BJT depending on the geometry and is nearly negligible in this design. The base current for bipolar transistors is $I_b = I_c/\beta$ with $\beta \approx 100$ for the technology used for these chips.
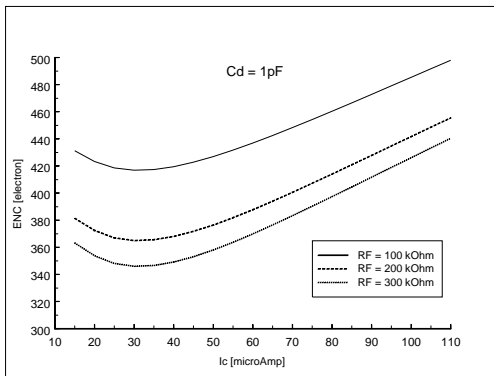
Figure 30: Equivalent noise charge as a function of collector current I_c for a detector capacitance C_d=1 pF
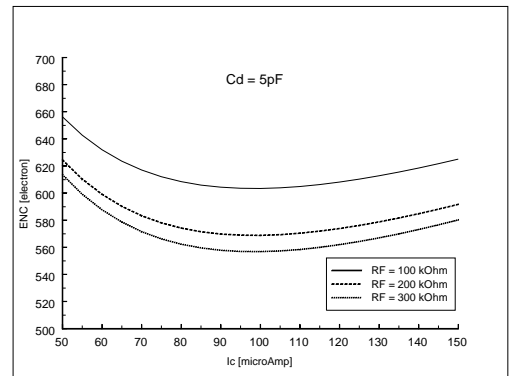
Figure 31: Equivalent noise charge as a function of collector current I_c for a detector capacitance C_d=5 pF

Calculations based on these simple formulae, but taking into account correlations between series and parallel noise contributions, have been performed [15]. Fig. 30 shows results for the example of $C_d = 1$ pF and an input transistor geometry optimised for this small capcitance. The solid line gives the equivalent noise charge for $R_f = 100$ kΩ and the dashed and dotted lines for $R_f = 200$ kΩ and $R_f = 300$ kΩ. In the case $R_f = 100$ kΩ the calculation gives an ENC of 420 electrons. This noise value is dominated by the relatively low value of R_f and later stage noise.

For an optimised front-end chip with $R_f \geq 200$ kΩ one expects an ENC of 350 electrons, which is a factor 2 improvement. Fig. 31 shows the case of C_d=5 pF, which is the maximum expected for a 6 cm long diamond detector, predicting a noise of 560 electrons. In order to obtain a signal-to-noise ratio of 14-to-1 for a diamond strip detector with 6 cm long strips, which will allow tracking with good efficiency, the diamond detector should deliver a most probable signal charge of about 7800 electrons.

5.3   Summary on Testbeam Results with SCT Readout

A CVD based diamond strip detector with 100 μm readout pitch has been tested with fast radiation hard readout electronics. As a readout chip the SCT32A with a peaking time of 25 ns was chosen. An equivalent noise charge of 656 electrons was measured for the SCT chip connected to the diamond after common mode correction. Track signals were reconstructed on the diamond yielding a spatial resolution of 36 μm and a mean signal-to-noise of 4.3. This result is in agreement with the expected value for this version of the chip connected to this diamond detector.

A calculation shows that the noise can be reduced with a modified feedback resistor adapted for the low capacitance of diamond detectors and an increase in the gain in the first stage. A signal-to-noise of 14-to-1 is predicted for CVD diamond detectors with 6 cm long strips which give a signal of 7800 electrons at the peak of the Landau distribution.

6 New Collaborators in 1996

During the course of the last year four new institutions joined the RD42 project. Two of these new groups specialise in materials science studies of highly resistive materials. This is a sign that the material we have produced as a result of the collaboration between our group and manufacturers is now recognised as being the highest quality available in the world. These and other groups are interested in performing detailed material studies with this high quality material.

The two new materials science groups are from LEPES/Grenoble and LENS/Florence together with the University of Florence. The Grenoble group specialises in studies of diamond surface structure. They are currently studying the properties of Molybdenum/Gold contacts on our detector material. It is their thesis that these contacts should yield a 10-20 % increase in signal size. They have tried to test this hypothesis on lower quality material but having larger charged particle induced signals is an enormous advantage when looking for small improvements in the carbide formed between the electrodes and the diamond. The group also has electron spin resonance equipment which is capable of detecting electrically active traps in the diamond. Studies of the most recently grown material, as well as material which has been irradiated are underway or planned for the near future. We hope to correlate the presence of charged traps with the charge collection distance of the material.

The Florence groups are capable of a wide range of materials tests. These include Deep Level Transient Spectroscopy and temperature stimulated current measurements, X-ray diffraction, electron spin resonance, RAMAN spectroscopy, time resolved photoluminescence and infra-red absorption. In the past the group has studied growth characteristics of thin films in their own growth reactors and their prime interest in joining RD42 was to be able to compare the results achieved on their own samples with those of the highest quality samples available. We have instituted a number of systematic studies using these probes over a wide range of collection distances (ranging from a few microns to more than one hundred microns) and a wide range of radiation doses. In particular we have begun a systematic study of the "pumped up" state in an effort to determine how this state differs from the "as-grown" condition. If we can pinpoint the differences we may be able to improve the growth processes, thereby gaining 60 to 80 % in collection distance.

In addition to these two groups we have been joined by two groups with more traditional particle physics backgrounds. The NIKHEF group has extensive expertise in the surface properties and charge transport mechanisms in highly resistive materials. This work was focused on understanding the behaviour of micro-strip gas chambers in their application to tracking in LHC experiments. The group has started to use laser stimulation of CVD diamond tracker prototypes to better understand the potential space charge limitations and surface charge distributions which might eventually be encountered with CVD diamond trackers in use at the LHC. The group is also interested in the eventual application of these detectors to trackers in the ATLAS experiment.

Finally, the GSI-Darmstadt group has been working with us for more than a year, however they only recently formalised their membership in the collaboration. Their interest in CVD diamond is two-fold. First, they require a series of radiation hard beam monitors to study and control the very intense heavy ion beams which are the heart of the new facility at GSI. At full luminosity a Uranium beam is expected to deposit 25 GRad in a 150 micron thick solid-state detector *every day*. In order to have any hope of localising the beam and optimising the performance of the accelerator they need homogeneous, radiation hard beam counters. The issue signal size is less important since heavy nuclei deposit Z^2 times as much charge per ion (where Z is the nuclear charge of the beam element) than singly charged particles of the same momentum. Preliminary studies show that the diamond quality already available is entirely
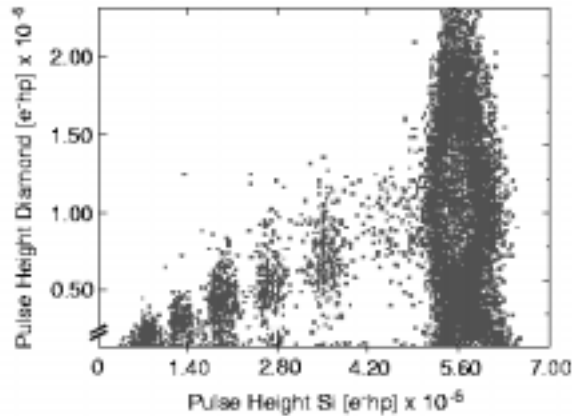
Figure 32: Fragmentation of ^{20}Ne ions measured in silicon and diamond.

suitable for these purposes. Work has now turned to a final optimisation of detector size and layout. The second goal of the GSI group is the application of diamond sensors to the detection of the heavy ion collision products. Here the issue of signal size returns as there are many singly charged particles in the final state. Studies have already been done which show nuclear fragments with $Z = 3$ to 10 are distinguishable in diamond detectors [Fig. 32]. Although the doses here are more modest, the detection of the decay products must still be done in a region were the radiation doses are expected to exceed those found in the heart of LHC experiments. RD42 stands to gain substantial experience in the radiation hardness of the material with which we are working as the GSI group extends its beam monitoring studies to higher intensity and higher Z beams. We will also gain experience in the use of larger area detectors by developing prototype beam monitors for this new application.

7 Proposed Research Program for 1997

Although tremendous progress has been made in the past year there remains a coherent set of detector R&D tasks to complete the work of the RD42 project over the next one and a half to two years.

While diamond material is very close to being suitable for use in an LHC tracker, having achieved a collection distance of 200 μm, it is essential to achieve more than 250 μm collection distance. It also has to be demonstrated that it is possible to achieve uniform collection distance over the whole detector surface of a big detector of about 30 cm^2 in order to provide usefull and reliable detector systems at very small distance from the interaction region. Such diamonds will have most probable signals above 7000 e assuring better than 12:1 signal to noise with fast rad-had electronics proposed above. This will be accomplished by (1) making a series of thick growths and post processing the diamond and/or (2) improving the chemistry. In addition, there remains the cost and feasibility questions associated with the growth of large quantities of this material. In the past we have been able to scale up production [16] but this has taken six months to a year. However, there is a bonus. In the process of scaling up production manufacturer's typically improve the material as the growth machines, presumably dedicated to the project, operate for long uninterrupted periods of time. The effort results in much more reliable CVD material. Coupled to the scaling up of production will be the production of a number of full LHC-scale particle detector prototypes.

Perhaps the most significant remaining obstacle to produce a prototype radiation hard tracking detector module is the absence of suitable electronics. Although the SCT32A has been used

30

to demonstrate the viability of diamond trackers at short shaping times a dedicated design in a radiation hard process will be necessary to exceed 12:1 signal to noise value in a full sized tracker module. We propose here to use the DMILL process with Matra MHS. This will take considerably more resources than we have been able to dedicate to electronics over the past three years. Efforts are however underway to combine this work with the development going on for silicon strip detector readout.

In addition to these two obvious, and largely parallel efforts, there remains the task of building, irradiating and testing detector prototypes. The experience we have gained with the metalisation of tracker and pixel patterns, the irradiation of small samples and the operation of small prototypes including very low noise analog readout electronics in testbeams leaves us in a strong position to carry out this effort.

We have demonstrated that we are now in the position to create the first full size, radiation hard LHC tracking detectors which will perform with more than 10 : 1 signal to noise at LHC shaping times and will last for more than ten years of trouble free LHC operation at small radii. We believe that the RD42 collaboration can most effectively do the specific prototyping work for each of the proposed LHC experiments. A fragmentation of this effort into the different experiments at this stage would be an enormous setback. We do, however, see this work will naturally evolve into an experimental design over the next 18 to 24 months.

8 Responsibilities and Funding for 1997

What follows is a breakdown of the areas of research that will be pursued at the different institutes (Table 3) involved in the project, a budget for the work to be carried out (Table **??**) and sources of funding expected for the project (Table **??**).

8.1 Requests from CERN Infrastructure

It is anticipated in addition to the funding needed to purchase diamond samples and develop radiation hard low noise electronics, that the following requests will be made on the CERN infra-structure:

- four 5-day testbeam running periods per year for the duration of the project;

- computing time and disk space on the central CERN computers;

- maintain the present 20 m^2 of laboratory space for test setups, detector preparation and electronics development;

- maintain the present office space for full time residents and visiting members of our collaboration;

8.2 Research Responsibilities

Institute	1	2	3	4	5	6	7	8	9	10	11	12	13	14	15	16	17	18
Diamond Character.		x	x			x	x			x	x					x		x
Meeting w/Companies											x					x		x
Radiation Hardness	x	x				x	x				x	x	x			x		x
Detector Design-LHC						x				x	x					x		
-HERA-B		x																
-Heavy Ion			x															
Rad.Hard Electronics						x					x				x	x		
Data Analysis	x		x			x	x			x		x						
Materials Studies				x	x				x		x		x	x		x	x	
Diamond Growth					x												x	

Table 3: Research Interests of groups involved (1=Vienna, 2=MPIK-Heidelberg, 3=GSI, 4=LENS, 5=Florence, 6=LEPSI, 7=Rutgers, 8=CPPM, 9=LEPES, 10=NIKHEF, 11=OSU, 12=Bristol, 13=LANL, 14=LLNL, 15=Pavia, 16=CERN, 17=Sandia, 18=Toronto).

9   Publications and Talks given by RD42

9.1   Publications

1. M. H. Nazaré *et al.*, "Development of Diamond Tracking Detectors for High Luminosity Experiments at the LHC", CERN/DRDC 94-21, DRDC-P56, May 1994.

2. R. Stone *et al.*, "Test of a Diamond-Tungsten Sampling Calorimeter", Mat. Res. Soc. Symp. **339** (1994) 121.

3. C. White *et al.*, "Correlations Between Electrical and Material Properties of CVD Diamond", Mat. Res. Soc. Symp. **339** (1994) 589.

4. R.J. Tesarek *et al.*, "Performance of a Diamond-Tungsten Sampling Calorimeter", Nucl. Instr. and Meth. **A349** (1994) 96.

5. A. Rudge, "Investigation of a Fast Amplifier with a Diamond Detector", Submitted to the Elba meeting (May 1994).

6. W. Dulinski *et al.*, "Diamond Detectors for Future Particle Physics Experiments", CERN PPE/94-222, submitted to ICHEP94, Glasgow, Dec. 1994.

7. C. White *et al.*, "Diamond Detectors for High Energy Physics", Nucl. Instr. and Meth. **A351** (1995) 381.

8. F. Borchelt *et al.*, "First Measurements with a Diamond Microstrip Detector", Nucl. Instr. and Meth. **A354** (1995) 318.

9. H. Pernegger *et al.*, "Radiation Hardness Studies of CVD Diamond Detectors", Nucl. Instr. and Meth. **A367** (1996) 207.

10. W. Dulinski *et al.*, "Results from CVD Diamond Trackers", Nucl. Instr. and Meth. **A367** (1996) 212.

11. C. Bauer *et al.*, "Pion Irradiation Studies of CVD Diamond Detectors", accepted for publication in Nucl. Inst. and Meth. (1996).

12. C. Bauer *et al.*, "Diamond Detectors at the LHC", accepted for publication in Nucl. Inst. and Meth. (1996).

13. D. Meier *et al.*, "Diamond as a Particle Detector", accepted for publication in Il Nuovo Cimiento (1996).

14. E. Berdermann *et al.*, "Diamond Detectors for Heavy Ion Measurements at GSI Darmstadt", to be published in the Proceedings of the 5th Int'l Conference on Advanced Technology and Particle Physics.

15. M.M. Zoeller *et al.*, "Performance of CVD Diamond Microstrip Detectors under Particle Irradiation", submitted to IEEE Transactions on Nuclear Science (1996).

16. C. Bauer *et al.*, "Proton Irradiation Studies of CVD Diamond Detectors", in preparation.

9.2   Talks

1. Beauty 94

2. Indiana Vertex Detector Workshop 94

3. Charm 2000 (FNAL)

4. Int'l Conference on HEP 94 (Glasgow)

5. Int'l Conference on New Diamond Science and Technology 94

6. APS/DPF 94 (2 talks)

7. COMO 94 (3 talks)

8. Diamond Films 94

9. Vienna Wire Chamber Conference 95 (2 talks)

10. Semiconductor Detectors (Schloss Elmau) 95

11. Vertex 95 (Israel)

12. Beauty 95

13. European Physical Society (Brussels) 95

14. IXth Int'l Workshop on Room Temperature Detectors 95

15. Hiroshima - Solid State Detectors 95

16. EuroDiamond 96 (Torino)

17. Radiation Effects on SemiConductor Detectors 96 (Florence) (2 talks)

18. Radiation Hardness Workshop 96 (Scotland)

19. Vertex 96 (Italy)

20. COMO 96 (4 talks)

21. IEEE 96

References

[1] C. Bauer *et al.* (RD42-Collaboration). "Development of Diamond Tracking Detectors for High Luminosity Experiments at the LHC". LDRB Status Report/RD42, CERN, (Oct. 1995). LHCC 95-43.

[2] C. Bauer *et al.* (RD42-Collaboration). "Addendum to Development of Diamond Tracking Detectors for High Luminosity Experiments at the LHC". LDRB Status Report/RD42 Addendum 2, CERN, (Nov. 1995). LHCC 95-58.

[3] M.A. Plano *et al.* "Thickness Dependence of the Electrical Characteristics of Chemical Vapor Deposited Diamond Films". *Appl. Phys. Lett.*, **64**:193, (1994).

[4] St. Gobain/Norton Diamond Film, Goddard Road, Northboro, MA 01532, USA.

[5] De Beers Industrial Diamond Division Ltd., Charters, Sunninghill, Ascot, Berkshire, SL5 9PX England.

[6] S. Zhao. "Characterization of the Electrical Properties of Polycrystalline Diamond Films", (1994). Ph.D. Dissertation, Ohio State University.

[7] M.H. Nazaré *et al.* (RD42-Collaboration). "Development of Diamond Tracking Detectors for High Luminosity Experiments at the LHC". RD42-Proposal, CERN, (May. 1994). DRDC 94-21/P56.

[8] W. Dulinski. "Electron Irradiation of CVD Diamond". RD42 Collaboration Meeting Notes, (Jun. 1995).

[9] S. Han *et al.* "Proton Irradiation Studies of CVD Diamond Detectors", (1996). in preparation for submission to NIM.

[10] C. Bauer *et al.* "Pion Irradiation Studies of CVD Diamond Detectors", (1996). Preprint CERN-PPE/95-173 accepted for publication in NIM.

[11] M. Edwards and D.R. Perry. "The Radiation Rardness Test Facility". *RAL Report*, RAL-90-065:p.21, (1990).

[12] F. Anghinolfi *et al.* "SCTA - A Radiation Hard BiCMOS Analogue Readout ASIC for the ATLAS Semiconductor Tracker", (1996). submitted to IEEE Trans. Nucl. Sci.

[13] M.Dentan *et al.* First Workshop on Electronics for LHC Experiments, (Oct. 1995). CERN/LHCC/95-56.

[14] W. Adam *et al.* (RD42-Collaboration). "Behaviour of CVD Diamond Strip Detectors in Magnetic Field". RD42 Internal Note 96-6, CERN, (Oct. 1996).

[15] W. Dabrowski *et al.* private communication.

[16] R.J. Tesarek *et al.* "Performance of a Diamond-Tungsten Sampling Calorimeter". *Nucl. Instr. and Meth.*, **A349**:96, (1994).